Ecological Modelling 301 (2015) 62–71

Contents lists available at ScienceDirect

Ecological Modelling

journal homepage: www.elsevier.com/locate/ecolmodel

From protein damage to cell aging to population fitness in *E. coli*: Insights from a multi-level agent-based model

Kameliya Z. Koleva, Ferdi L. Hellweger*

Department of Civil and Environmental Engineering, Northeastern University, Boston, MA, USA

ARTICLE INFO

Article history:
Received 7 August 2014
Received in revised form 6 January 2015
Accepted 25 January 2015

Keywords:
Protein damage
Aging
Fitness
Bacteria
Agent-based model

ABSTRACT

Aging is an important process affecting many organisms, including bacteria that appear to divide symmetrically. Recent research has established much of the mechanisms underlying aging in *Escherichia coli*, including the role of damaged protein aggregates (DPAs) that are transported by diffusion within the nucleoid-free intracellular space, which leads to their polar localization and asymmetric inheritance (i.e. aging). This provides an opportunity to develop a mechanistic model of *E. coli* and use it to assess the role of this process at the population level. Is there a fitness benefit to asymmetric inheritance of DPAs? Here we explore this question using a multi-level agent-based model, which simulates a population of individual cells, each with a population of individual DPAs. The model is compared to relevant data compiled from four published studies, which shows it reproduces the main patterns observed, including intracellular localization and inheritance of DPAs, their effect on growth rate, differences in growth rate between sibling pairs, under unstressed and heat shock conditions, for wild type and a mutant that partitions DPAs symmetrically. The model is used to estimate population growth rates of the wildtype and mutant, which shows a statistically significant benefit of aging by asymmetric DPA segregation. However, the benefit is very small and probably not relevant in the context of the ecology of the bacteria's primary habitat (the intestinal tract of warm-blooded animals). But, at an evolutionary time scale even this small benefit may be relevant for bacteria with large population sizes and short generation times.

1. Introduction

Aging is an important process affecting both multicellular and unicellular organisms (Kirkwood, 2005), which makes understanding the ecological role of this process an important research subject. It can be defined as a decrease in reproductive and increase in mortality rate with age. This can be due to damage accumulation which, in aging organisms, is asymmetrically inherited. One individual ("parent") inherits more damage than the other ("child"). Non-aging organisms segregate the damage symmetrically and keep it from accumulating by degradation, repair and/or growth dilution. Asymmetric inheritance and degradation/repair/dilution are alternative strategies for coping with damage, but they are not mutually exclusive. An important question relates to the role of aging in the ecology of an organism. Does it constitute a fitness benefit or cost? A simple example can illustrate how it may be beneficial to segregate the damage asymmetrically. Consider two populations with the same total amount of damage but differently distributed among the individuals. If the effect of damage on the growth rate saturates at higher damage, then a population with a homogenous distribution will have a lower population-average growth rate than a population with a heterogeneous distribution (i.e. one that ages).

Until recently it was not clear that bacteria age and work in this area has thus focused on higher organisms, like the budding yeast *Saccharomyces cerevisiae* (Erjavec et al., 2007; Sinclair, 2002). However, we now know that bacteria also age (Ackermann et al., 2003; Stewart et al., 2005). This allows us to employ these model organisms (especially *Escherichia coli*), which have helped us understand so many other mechanisms underlying life, to also learn about aging. Further, there is increasing realization of the importance of intestinal bacteria (including *E. coli*) to human health, and understanding the fitness and ecology of the gut microbiome is an important contemporary problem (Consortium, 2012; Stein et al., 2013).

1.1. Aging in E. coli

It was not always clear if bacteria that divide by apparent symmetric division, including *E. coli*, age. Although about 50 years ago, Powell and Errington (1963) manually monitored bacteria under

* Corresponding author. Tel.: +1 617 373 3992; fax: +1 617 373 4419.
E-mail address: ferdi@coe.neu.edu (F.L. Hellweger).

http://dx.doi.org/10.1016/j.ecolmodel.2015.01.024
0304-3800/

a microscope and found higher generation times of "outer" over "inner" sisters. The number of observations in that study was relatively small and the effect was statistically significant in only one of two *E. coli* datasets. More recently, Stewart et al. (2005) used automated time-lapse microscopy, which allowed them to track many more cells. They conclusively demonstrated that the offspring that inherits the old pole has a lower growth rate. Subsequent work in this area has focused on understanding the mechanisms underlying this aging process. Lindner et al. (2008) followed damaged protein aggregates (DPAs) via fluorescently tagged IbpA chaperone protein, which associates with the DPAs. They found that DPAs localize at the poles and that asymmetric inheritance of DPAs can explain part of the observed aging. The remainder is attributed to an other old pole (OOP) age effect, due to an unknown mechanism. Winkler et al. (2010) studied DPAs in heat-stressed and unstressed wild type and various mutants (e.g. one that inherits DPAs symmetrically) using fluorescence microscopy of thermolabile reporter and various chaperone proteins, EM tomography and other techniques. They also observed polar localization of DPAs and lower growth rates of old pole cells. An individual-based model (IBM, aka agent-based model, ABM) of DPAs, with passive diffusion and nucleoid occlusion processes was able to reproduce the polar localization. Saberi and Emberly (2010) also present an ABM that can explain polar localization of DPAs by aggregation and nucleoid occlusion. Most recently, Coquel et al. (2013) used time-lapse fluorescence microscopy, automated image analysis and ABM to track individual DPAs and established that their transport is by diffusion. Their ABM, based on diffusion and nucleoid occlusion, reproduces observed localization of DPAs.

These studies were all done with *E. coli* growing on agar plates. Wang et al. (2010) grew *E. coli* in a microfluidic device and did not observe a decrease in growth rate. They suggest the difference between their and previous results may be due to experimental conditions. Their experimental set-up allowed them to monitor single cells over hundreds of generations, which revealed an increase in death rate with age. Also, although there are now numerous reports to support passive transport of DPAs (Coquel et al., 2013; Saberi and Emberly, 2010; Winkler et al., 2010), Rokney et al. (2009) found the transport to be energy-dependent. The reason for the difference is not clear, and Winkler et al. (2010) points to some experimental details.

The past research summarized above does not establish a complete or consistent mechanism for aging in *E. coli*. Further experimental work is needed to understand why we see aging under one condition but not another. However, for growth on agar plates there is consistent evidence that *E. coli* age via a DPA-related mechanism (Fig. 1), which is what we will focus on here.

1.2. Modeling aging of microbes

Several models have been developed and used to investigate the ecological role of aging in microbes (Ackermann et al., 2007; Chao, 2010; Johnson and Mangel, 2006; Rang et al., 2011; Watve et al., 2006). For example, Watve et al. (2006) developed a matrix model that simulates cells with a number of growth-limiting components that are subject to aging, affect the cell growth rate and are segregated in a symmetric or asymmetric manner at division. Ackermann et al. (2007) presented an ABM of individual cells that accumulate and degrade damage, which affects the survival and/or fertility (i.e. growth rate) and is inherited with variable degree of symmetry. These models support a fitness benefit of asymmetric damage segregation under a wide range of conditions. Most recently, Clegg et al. (2014) presents a model that includes repair of damaged proteins to functional proteins, and that model suggests that repair (vs. asymmetric inheritance) of damage is the better strategy.

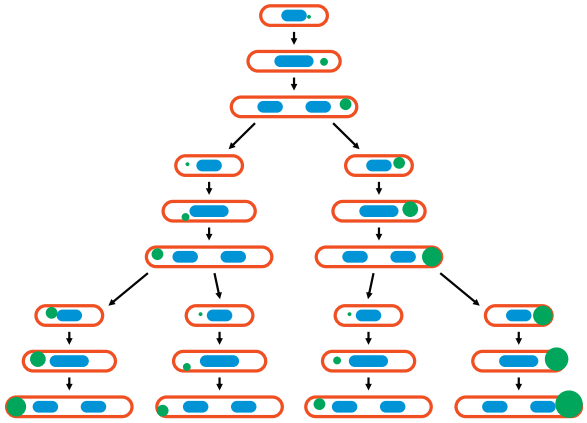

Fig. 1. *E. coli* aging via damaged protein synthesis, aggregation, diffusion and segregation. Red = cell, blue = nucleoid, green = damaged protein aggregate (DPA). The cells shown follow the typical aging life history, where the initial appearance of DPAs is symmetric, but skewed towards the old pole after one or more divisions. Other possible cases, like multiple DPAs, mid-cell localization of DPAs and DPAs switching locations are not shown. (For interpretation of the references to color in this figure legend, the reader is referred to the web version of this article.)

These models are all relatively simple and describe the underlying mechanisms in general terms (e.g. damage accumulation), which means they are easy to understand and can be used to reach general conclusions. However, their simplicity also limits their representation of specific mechanisms. It is unclear what parameters or equations describing damage accumulation/degradation/segregation are representative of DPAs in *E. coli*. Can these mechanisms even be captured by these simple equations? For example, none of the existing models explicitly considers the aggregation of damage and heterogeneity of DPA sizes. This is likely a key feature of the overall aging mechanism, because smaller DPAs diffuse freely from pole to pole and are inherited symmetrically, whereas larger DPAs are constrained by the nucleoid and divide asymmetrically. A number of more mechanistically detailed models of DPA aggregation and localization in *E. coli* have recently been developed, but they do not extend beyond the cell level and cannot be used to estimate population growth rates (Coquel et al., 2013; Saberi and Emberly, 2010; Winkler et al., 2010).

1.3. Question and overview of approach

Here we aim to explore and quantify the ecological fitness benefit of DPA-related aging in *E. coli* growing on agar plates. For this specific case, ecological fitness can be quantified as the population growth rate. Does asymmetric inheritance of DPAs increase the population growth rate? By how much? The existing data provide much insight into the underlying mechanisms, but they cannot be used directly to answer these questions. Our strategy is to develop a model of *E. coli* including the mechanisms needed to reproduce relevant observed patterns (e.g. growth rate differences between sibling pairs, DPA localization the cell). This general approach for the analysis of complex systems has been referred to as pattern-oriented modeling (Grimm et al., 2005). Then we use the model as an experimental system to quantify the benefit of this trait. Specifically, we simulate colonies of aging wild-type and non-aging mutant strains and estimate their population growth rates. Compared to most previous models of aging in microbes, our model is relatively specific (i.e. *E. coli*, on agar plates, DPA-related aging) and can be considered a "tactical" model (*sensu* (Evans et al., 2013)).

The problem at hand is challenging from a modeling perspective, because it involves the role of intracellular mechanisms in

the aging process at the population level. It covers two levels of biological organization. Crossing these scales can be achieved in a relatively straightforward manner using an agent-based approach for cells and adding more complex intracellular mechanisms, as has been done for chemotaxis (Bray et al., 2007), circadian rhythms (Hellweger, 2010) and cell-to-cell communication (Rudge et al., 2012). However, these past models still use the conventional concentration-based, differential equation approach for simulating intracellular mechanisms. In this case, the intracellular population of DPAs is heterogeneous in size, which affects their behavior (e.g. diffusion past the nucleoid) in a non-linear manner and a key mechanism is inheritance of a single, discrete large DPA. These features are difficult to capture with differential equations, but straightforward to implement in an agent-based model. Previous models of this process were built using agent-based methods (Coquel et al., 2013; Saberi and Emberly, 2010; Winkler et al., 2010). Here we simulate a population of individual cells, each with a population of individual DPAs, a multi-level agent-based approach.

We present the model and compare it to relevant experimental data from the literature, which shows that it is consistent with the main observed patterns. Then we use the model to explore the role of asymmetric DPA segregation in the fitness (i.e. population growth rate) of the bacteria. Simulations with and without asymmetric DPA inheritance show a small but statistically significant ecological benefit to aging, although it is probably not experimentally observable or relevant in the ecology of the gut. However, considering large population size and short generation time of bacteria, it may be relevant from an evolutionary perspective.

2. Model description

2.1. Overview

The model simulates individual cells as spherocylinders that grow, divide and shove each other. Inside the cells, the model simulates the nucleoid and a number of DPAs. Damaged proteins are generated continuously, move about the cell (outside the nucleoid) and aggregate when they meet. They are degraded and inherited by offspring. The cell growth rate is affect by DPA and OOP effects (see below).

2.2. Cells

A number of spatially-explicit ABMs of bacteria have been developed that represent cells as spheres (Kreft et al., 1998), spherocylinders (also referred to as capsules or pills) (Melke et al., 2010; Rudge et al., 2012; Volfson et al., 2008) or flexible or elastic rods (Grant et al., 2014; Janulevicius et al., 2010). Here, cells are represented as spherocylinders with constant radius. They grow by elongation at a biomass-based specific growth rate (μ, d^{-1}), meaning the biomass (m, g cell^{-1}) changes at a rate proportional to the biomass ($dm/dt = \mu m$).

The growth rate is a function of two aging mechanisms. DPAs account for only a fraction (e.g. ~30% in the experiments of Lindner et al. (2008)) of the difference in growth rates between sibling pairs, and the remainder is attributed to the other old pole (OOP) effect. Therefore, we calculate the growth rate by reducing the maximum growth rate (μ_m, d^{-1}) based on DPA (f_d) and OOP (f_p) effects using $\mu = \mu_m\,(1 - f_d - f_p)$. For the DPA effect, observations of Lindner et al. (2008) suggest the damage effect saturates (see Section 3). A number of different formulations, including making the effect a function of the mass of DPAs, were evaluated but could not reproduce the observed pattern using our model. Therefore, the DPA effect is modeled as a function of the total surface area of DPAs in the cell ($f_d = K_d\,\Sigma a_a$), where K_d (μm^{-2}) is the damage effect constant and a_a (μm^2) is the DPA surface area. The actual mechanism of DPA action is unknown, but there are several mechanisms that are consistent with the activity being proportional to surface area, like adsorption of a nutrient on the surface or consumption of energy by enzymes operating on the surface (see below). Since damaged proteins aggregate (see below) the specific surface area decreases with the number of damaged proteins and the damage effect saturates. Previous models of aging use different formulations for damage effect, including a saturating equation (Erjavec et al., 2008). The OOP effect is a function of the old pole age (a_p, which is 1 for a daughter cell inheriting the new pole of the mother). Specifically, $f_p = 0$ for $a_p = 1$, $f_p = f_{p,a}$ for $a_p = 2$ and $f_p = f_{p,a} + (a_p - 2) f_{p,m}$ for $a_p = 3+$. The OOP effect increases in a linear manner (i.e. does not saturate) and for very old cells, those with old pole ages of 34+ divisions, results in a negative growth rate. It is plausible that very old cells cease to grow completely. However, this is not realized in the relatively short simulations presented here (up to 9 generations). This approach to modeling aging is simplified and the actual mechanisms are undoubtedly much more complex. However, it is based on reasonable assumptions and comparison to observations (see Section 3) show that it produces aging patterns consistent with observations.

A cell divides when it reaches a specified size ($l_{c,d}$, μm). The mother cell mass is divided between the two daughter cells using a specified new-pole offspring split fraction (sf_n), which can be assigned different from the ideal 0.5 to account for division asymmetry (Stewart et al., 2005). In addition, the split fraction is varied stochastically by drawing from a truncated (to avoid unrealistic values, e.g. split fraction >1.0) normal distribution (Hellweger, 2013; Kreft et al., 1998). The aging (DPA and OOP effects) and division (split fraction) mechanisms produce heterogeneity. However, there are other sources of heterogeneity, like stochastic gene expression (Pedraza and van Oudenaarden, 2005), and those are accounted for by varying the maximum growth rate (μ_m). The maximum growth rate of each cell is assigned at division by drawing from a truncated normal distribution. This process simulates phenotypic heterogeneity (vs. heritable), so the values are drawn from a global distribution (vs. one that has the mother cell value as the mean). A similar approach, with proper accounting for mutation rates and tradeoffs, could be used to simulate evolution, but that is unlikely to be a factor in the applications presented here. The age of the cell poles changes at division in a deterministic manner. A mother cell with pole ages $(0, 1)$ divides into daughter cells with pole ages $(1, 0)$ and $(0, 2)$. A mother with ages $(0, 2)$ divides into daughters with ages $(1, 0)$ and $(0, 3)$.

Cells interact by shoving each other. Contact is simulated using the method of viscoelastic virtual spheres (Volfson et al., 2008). Consider two cells, potentially in contact. A virtual sphere with the same radius as the cell is positioned inside each cell at the closest point to the other cell. If the spheres overlap the cells are in contact. The force between the spheres is calculated based on the overlap distance and a spring constant (k_f, N), and the resulting force and torque on the cells is computed based on that. An additional small random force (r_f, N) and torque (r_t, N m) is applied to each cell to avoid cells forming one long single-file colony. Cell displacement is based on the sum of all forces and torques acting on the cell. Movie S2 illustrates cell shoving and virtual spheres. This cell-to-cell interaction does not affect the growth or aging of individual cells or the colony. However it allows us to simulate colony growth on a petri dish and generate pictures and movies of the spatial configuration of cells and DPAs, which help understand the behavior of the model (e.g. diffusion of DPAs of different sizes, see Section 3.2) and can be compared to observations (see Fig. 2B). The feature may also be useful in future modifications or applications of the model.

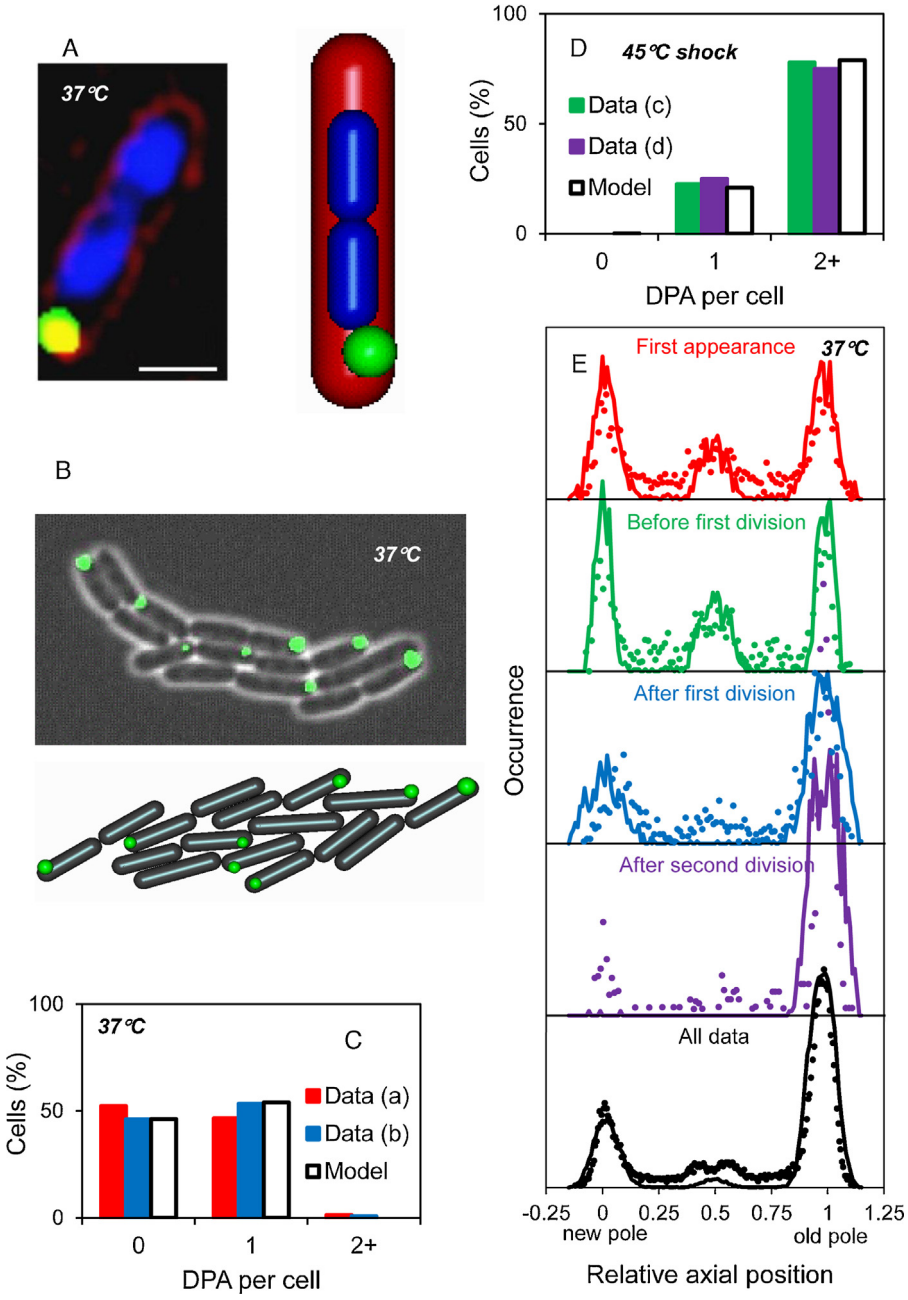

Fig. 2. Model-data comparison for DPA localization. (A) Typical spatial configuration of nucleoid and damaged protein aggregates (DPAs) inside the cell. Red = cell, blue = nucleoid, green = DPA. Left = data, right = model. Scale bar: 1 μm. DPA radius exaggerated ×5. See Movie S4. (B) Typical colony of cells with DPAs. Gray = cells, green = DPA. Top = data, bottom = model. See Movie S3. (C) DPAs per cell under unstressed conditions. (D) DPAs per cell under heat shock conditions. (E) Axial distribution of DPAs at various times in the division cycle. Symbols are data and lines are model. Data sources: Panels A, B, C (a), E from Lindner et al. (2008), C (b) from Coquel et al. (2013), D from Winkler et al. (2010). Data images in panels A and B copyright © (2008) by the National Academy of Sciences. Model detection limit for DPAs is 7000 proteins DPA^{-1}. (For interpretation of the references to color in this figure legend, the reader is referred to the web version of this article.)

2.3. Nucleoid

Various approaches have been used to model the nucleoid, including specifying a repulsive velocity potential (Winkler et al., 2010), immobile obstacles (Coquel et al., 2013) and dynamically simulating the DNA molecule as a circular polymer (Saberi and Emberly, 2010). Here, the nucleoid is modeled as one or two spherocylinders. The spherocylinders have a specified radius (r_n) and the length increases with cell growth. The nucleoid occupies a constant fraction of the cell volume (f_n). When the absolute volume reaches a threshold ($v_{n,d}$, as the cell becomes larger and approaches division), the nucleoid is present as two spherocylinders. The dynamics of the nucleoid are apparent in Movie S4.

2.4. Damaged protein aggregates (DPAs)

Past microbe aging models use varying approaches to simulate damaged proteins (for a more thorough review, see Clegg et al. (2014)). For example, the model of Erjavec et al. (2008) tracks intact and damaged proteins, where intact proteins are converted to damaged proteins, and both types degrade in a first-order manner. The model of Ackermann et al. (2007) includes generic damage, which

may include oxidized protein, that is generated at a constant rate and can be removed at a cost to the cell's survival probability. Clegg et al. (2014) include active and damaged protein. Active protein becomes damaged, but can be repaired back to the active form by a fraction of the active protein that does not contribute to cell growth. Here we use a relatively simple approach, where damaged proteins are generated, aggregate and are degraded (see next paragraph). Comparison to observations (see Section 3) suggests this simplified approach is sufficient to reproduce the major observed patterns of DPA accumulation and effect on growth of *E. coli*.

DPAs are simulated using an agent-based approach. Damaged proteins are added continuously at a constant damage rate (k_d, proteins min^{-1}) and positioned randomly within the cell cytoplasm outside of the nucleoid. The damage rate can be changed to account for different temperatures, including heat shock. Transport and aggregation is based on previous models by Winkler et al. (2010) and Coquel et al. (2013). The radius of a DPA (r_a) is a function of the number of proteins making up the DPA (n_a) using $r_a = n_a^{1/3}\ r_p$. DPAs are transported by random walk with a diffusion coefficient (D_a), calculated from that of a monomeric protein (D_p) using $D_a = D_p\ (r_p/r_a)$. DPAs cannot overlap the nucleoid or cell wall, so larger DPAs are more confined. In addition, DPAs are advected outwards based on the cell elongation rate and inherited by daughter cells at division. Inheritance is based on the DPA's position in the mother cell. For the case where DPAs were re-localized to the inner membrane (see Section 3) (Winkler et al., 2010), the DPAs are inherited with equal probability by the offspring. When two DPAs meet (their separation distance is less than r_p) they combine to form a larger DPA. Individual damaged proteins are degraded by at removal rate ($k_{r,a}$, min^{-1}) that varies by the DPA's specific surface area (sa_a, μm^{-1}) using $k_{r,a} = k_{r,p}\ (sa_a/sa_p)$, where $k_{r,p}$ (min^{-1}) and sa_p (μm^{-1}) are the removal rate and specific surface area of monomeric proteins, respectively. It is plausible that degradation of repair mechanisms operate at the surface of the DPA, so that the rate is higher for smaller DPAs with higher specific surface area. The process is simulated in a stochastic manner (e.g. the probability of a protein being degraded in any given time step is $k_{r,a}\ \Delta t$).

Simulating each protein as an individual agent can be very computationally demanding. The model therefore includes a simplification, where only DPAs above a certain threshold ($n_{a,0}$, proteins DPA^{-1}) are simulated. The DPAs below the threshold are assumed to be small enough to diffuse freely within the cell. That means they are uniformly distributed, divide symmetrically and affect the growth rate of all cells equally. Their effect is therefore constant and implicitly accounted for in the maximum growth rate parameter. With an appropriate adjustment in the removal rate, this approximation produces a similar pattern of protein accumulation and aggregation (see Fig. S1). These types of approximations are common in agent-based modeling. Agent-based models of microbes commonly simulate a smaller number of representative cells called super-individuals (Bucci et al., 2011; Fredrick et al., 2013; Hellweger, 2010, 2013).

2.5. Parameter values

The model includes 21 parameters, which were assigned values consistent with the literature (where available, Table S1). Several parameters are not constrained well by the available literature and they were calibrated to match the observations (Figs. 2 and 3, discussed later). The amount of protein damage and size of DPAs is uncertain. Stressed cells have been observed to contain 1.5–3% damaged proteins, which are present in aggregates with 2.4×10^3–1.7×10^4 proteins DPA^{-1} (Winkler et al., 2010), corresponding to a DPA radius of 4.0×10^{-2}–7.6×10^{-2} μm (see conversion above). In unstressed cells, the number of aggregated proteins is lower, observed at ≤0.5% (Mogk et al., 2003). However, DPAs in unstressed cells were estimated, based on diffusion characteristics, to have a radius of 5.4×10^{-2}–2.7×10^{-1} μm, which corresponds to 5.8×10^3–7.5×10^5 proteins DPA^{-1}. The protein damage and removal parameters (k_d, $k_{r,p}$) were adjusted so that the model produces an average maximum DPA size of about 1×10^4 proteins DPA^{-1}, which seems a reasonable value. Related to the DPA size, there is considerable uncertainty about the nucleoid radius, which along with the inner cell radius, controls DPA diffusion past the nucleoid. In reality, the extent of the nucleoid is not defined by a discrete boundary (i.e. as it would be for a membrane-bound nucleus), but it is diffuse. Other approaches that explicitly simulate the DNA polymer may be more realistic (Saberi and Emberly, 2010). Here, the nucleoid volume fraction (f_n) and radius (r_n) and the inner cell radius ($r_{c,i}$) were adjusted to match the observations of DPA localization. The model is applied to a number of datasets from experiments with different strains and experimental conditions. Some experiments with similar setup produce different results. For example, growth rate differences of sibling pairs at 30 °C were found by Stewart et al. (2005) for MG1655 to be ~5% after seven consecutive old/new pole division, whereas Winkler et al. (2010) with modified MC4100 found ~10% after four generations. To account for these differences we vary the parameters for the other old pole effect by strain ($f_{p,m}$, see Table S1).

2.6. Statistical significance testing

To test if asymmetric DPA inheritance is beneficial, we compare the mean growth rate from the model with asymmetric DPA inheritance to that from the model with symmetric DPA inheritance. The model is stochastic and we base the statistical significance of the results on a two-sample, one-tailed *t*-test. The model-predicted growth rates are normally distributed (see Fig. S2). The null hypothesis is that the aging strain does not have a larger growth rate than the non-aging strain. Statistical significance refers to $p < 0.05$.

3. Results and discussion

3.1. Model is consistent with observed patterns

The model was compared to relevant data compiled from four published studies (Coquel et al., 2013; Lindner et al., 2008; Stewart et al., 2005; Winkler et al., 2010). These studies do not include the conflicting reports of no aging and active DPA transport (Rokney et al., 2009; Wang et al., 2010), as discussed above. The comparison shows that the model reproduces the main observed patterns qualitatively and quantitatively (Figs. 2 and 3). This includes spatial patterns of intracellular DPAs and cells (Fig. 2A and B), and the number of cells with zero, one and more DPAs under unstressed (Fig. 2C) and heat shock (Fig. 2D) conditions. The higher number of DPAs under heat shock is reproduced by the model using a higher protein damage rate (see above). The model also captures the distribution of DPAs along the cell axis at various times, including the symmetric initial position and asymmetric, old-pole localization after divisions and over the entire experiment (Fig. 2E). Consistent with observations, the model shows DPAs along the entire cell axis with a minor peak at the center. In the model this feature is due to the larger nucleoid-free volume at the cell center when the nucleoid divides prior to division (see Fig. 2A and Movie S4). However, the model underestimates the magnitude of this peak, which may be due to the simplified representation of the nucleoid (see above). There is a correlation between damage and growth rate, with old-pole cells having higher damage and lower growth rates, a pattern that is reproduced by the model (Fig. 3A). Note that observations and model both show a saturating effect of damage

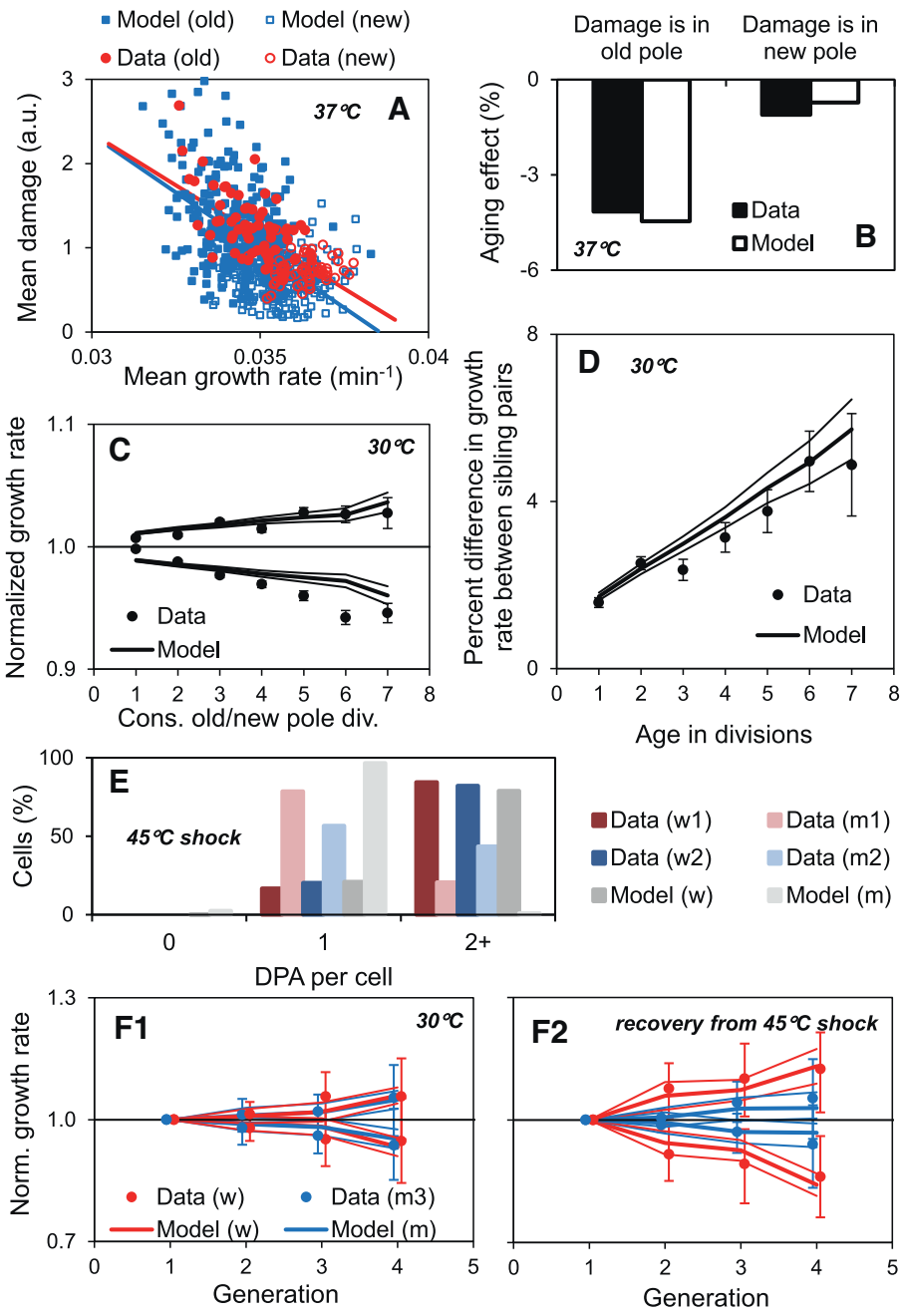

Fig. 3. Model-data comparison for DPA effect. (A) Correlation between damage and growth rate. Lines are linear regressions to all points (old and new pole). R^2: Data = 0.49, model = 0.28. (B) Effect of DPA inheritance on aging (see text). (C) Growth rate of new/old pole cells as a function of consecutive old/new pole divisions. (D) Growth rate differences of siblings as a function of mother old pole age. Error bars are ±1 standard error of the mean. (E) DPAs per cell of two strains under heat shock. w = functionally unaltered, m = no nucleoid. (F) Growth rate of new/old pole cells vs. generation. w = functionally unaltered, polar localization of DPAs (YFP-Luciferase), m = membrane-anchored, random localization of DPAs (2TM-YFP-Luciferase). Error bars are ±1 standard error of the mean. Data sources: Panels A and B from Lindner et al. (2008), C and D from Stewart et al. (2005), E and F from Winkler et al. (2010).

on growth rate (at higher damage the growth rate is higher than predicted by a linear model, the regression line). By comparing the growth rates of old/new pole offspring that do/do not inherit the DPA, the relative effect of the DPA vs. OOP mechanism can be determined. When the old pole cell inherits the DPA, the aging effect is larger (OOP + DPA) than when the new pole cell inherits the DPA (OOP – DPA). The model captures this behavior qualitatively and quantitatively (Fig. 3B).

The growth rate of the new pole offspring is higher than that of the old pole offspring, and this difference increases with the number of consecutive old/new pole divisions or age (Fig. 3C and D). The model reproduces this general pattern but it has less variability, which is expected considering that some variability in the data can be attributed to observational error, which is not included in the model.

To investigate the effect of the nucleoid on DPA localization, Winkler et al. (2010) exposed a number of different strains to heat shock. The functionally unaltered strain (labeled "w") has mostly two DPAs per cell (Fig. 3E, as seen previously in Fig. 2D). Two functionally altered strains that do not have a nucleoid (labeled "m1" and "m2") have mostly one DPA per cell. The model reproduces this feature, as does the model of Winkler et al. (2010).

To understand the role of asymmetric damage inheritance in aging, Winkler et al. (2010) performed experiments with two strains (Fig. 3F). The unaltered strain (labeled "w") localizes DPAs to the poles. The altered strain (labeled "m3") produces a molecule that attaches to the inner membrane and serves as aggregation seed for the DPAs. In these cells, DPAs are randomly distributed. At low temperatures, the experiments of Winkler et al. showed a larger aging effect (sibling growth rate difference vs. generation) compared to those of Stewart et al. (Fig. 3F1 vs. C), which may be due to different experimental methods and/or strains used. As discussed above, the parameters controlling the OOP effect were adjusted to reproduce these results (see Section 2.5). The unaltered and altered strains show a similar aging effect, presumably because the amount of damage is low, consistent with the low temperature (30 °C vs. 37 °C in the experiments of Lindner et al. (2008)). When the strains are exposed to heat shock to induce DPA formation and growth is observed in the recovery phase, the two strains produce different results (Fig. 3F2). At heat shock temperatures, the damage becomes larger (damage rate increases with temperature, see above) and that translates into a larger aging effect in the unaltered strain, which is carried over into the recovery phase. The strain with random DPA inheritance does not see an added aging effect, because the damage affects both offspring equally. The model produces results consistent with these observations.

Turning individual mechanisms on/off to investigate their role in the biology of an organism is a powerful tool, and it can be done experimentally using organisms like *E. coli*. Mechanistic models can simulate these perturbations and this allows for quantitative testing of a hypothesis. For example, the model of Winkler et al. (2010) (and ours) simulate DPA diffusion and aggregation in cells with and without nucleoid. The models reproduce the observed patterns in both strains, which provides evidence for the passive diffusion and nucleoid occlusion mechanisms. By simulating a population of cells, the model presented here extends up one level of organization and it allows for exploration of the role of a mechanism at the population level (i.e. aging). This approach was also used previously to explore the role of various mechanisms in producing heterogeneity in intracellular nutrient content in phytoplankton (Fredrick et al., 2013).

The model was designed to be consistent with the observed patterns and the model-data comparison above confirms that it behaves as designed. This comparison is important, because it is based on emerging behaviors of the model, not imposed rules (Grimm et al., 2005). For example, the DPA localization along the cell axis (Fig. 2E) was not imposed by some distribution rule (e.g. a multi-model Gaussian distribution), but emerges from the underlying mechanisms, like diffusion and aggregation. In our experience it is often difficult to predict how an individual mechanism affects the emergent behavior of these complex systems models. For example, in this project we tried multiple functions relating DPA to growth rate (see Section 2.2), several of which were not able to reproduce the observed patterns (Fig. 3A).

3.2. Model illustrates features not observed in experiments

A key mechanism in the model is the diffusion and aggregation of DPAs. The dynamics of the larger DPAs has been observed by Coquel et al. (2013) using time-lapse fluorescence microscopy, but this technology does not detect the smaller DPAs. The model can illustrate this feature. Movie S5 shows the intracellular distribution of all DPAs simulated (above a threshold, see model description), including those below the detection limit. It shows how DPAs migrate freely between poles, until they become too large to diffuse past the nucleoid. This is an important part of the aging mechanism in the model. The ability to visualize features not experimentally observable is a key attribute of a mechanistic model.

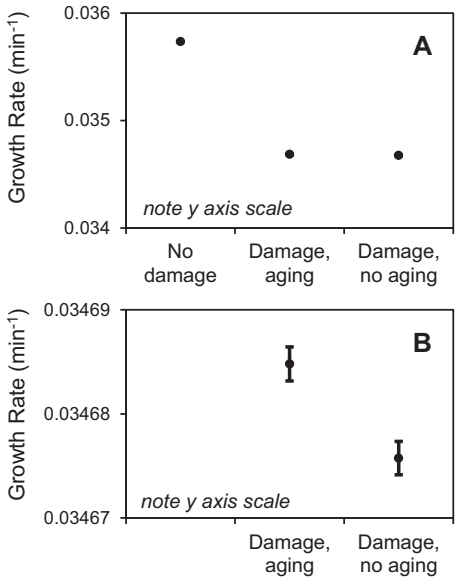

Fig. 4. Fitness effect of DPA damage and asymmetric segregation. "No damage" is the base case model with zero damage rate. "Damage, aging" is the base case model. "Damage, no aging" partitions DPAs symmetrically. Error bars are standard error of the mean. Panels A and B have different *y*-axis scales. Individual growth rates are provided as Table S2.

3.3. Asymmetric DPA segregation enhances ecological fitness

We next use the model to explore the ecological role (cost or benefit) of aging, specifically asymmetric inheritance of DPAs since that is the mechanism the model explicitly resolves. We quantify the effect by comparing the population growth rate of the wildtype and the mutant that partitions DPAs symmetrically (see above). The comparison is based on population growth rates, which result from the growth of individual cells of various ages, which is different from the comparison of aged vs. young cells within a population (Fig. 3C, B, D, and F). Note that the strains differ in the DPA effect, but age in the same way by the other old pole (OOP) effect, so this analysis does not quantify the total aging benefit/cost. Winkler et al. (2010) measured the growth rate of these two strains under unstressed (30 °C) and recovery from heat shock (30 °C after 20 min at 45 °C) conditions and found the aging strain to have higher growth rates (the experiments presented in Fig. 3F). For unstressed conditions the effect is small and not statistically significant (0.0240 ± 0.005 vs. 0.0238 ± 0.004 min^{-1}, mean ± standard deviation, $p = 0.25$), which may be a consequence of the relatively small sample size and low damage rate at this temperature. In recovery from heat shock, the effect is larger and statistically significant (0.0231 ± 0.006 vs. 0.0217 ± 0.005, $p = 0.000046$). However, neither of these experiments reflects the ambient conditions in the primary habitat of this species (i.e. the gut at 37 °C). Here we repeat these experiments numerically (i.e. we simulate them using the model) at 37 °C. To increase the accuracy, we simulate 5000 colonies with up to 512 cells, providing 2.6×10^6 individual growth rates.

Fig. 4 shows the resulting growth rates. To put the results into perspective we also show the growth rate of a strain that does not incur protein damage. The strains with protein damage grow slower, but their difference is very small (0.034685 ± 0.002615 vs. 0.034676 ± 0.002568). Nonetheless, the large number of samples allows us to conclude that the aging strain has a statistically significantly higher growth rate than the non-aging strain ($p = 0.000040$). The difference between the growth rates (selection rate constant (Lenski et al., 1994)) is 0.013 day^{-1} and their ratio (relative fitness (Lenski and Travisano, 1994)) is 1.00026. The relative fitness

with respect to the strain without protein damage of the aging and non-aging strains are 0.97059 and 0.97034, respectively, and the difference between those values is 0.00025. Using a different modeling approach, also parameterized based on data from Stewart et al. (2005), Chao (2010) also found a benefit to aging, but the difference in relative fitness was only 0.00003.

It is theoretically possible to confirm these results using the strains of Winkler et al. (2010), but the difference in growth rates may be too small to detect experimentally. Estimating growth rates from individual cells on a petri dish would require many observations, more than for a model simulation because the experiments would be subject to experimental noise. A more practical approach would be to perform competition experiments, which would intrinsically average out the growth rate of many cells. Lenski et al. (1994) used 6-day periodically diluted (daily, 1:100) competitions to detect growth rate differences of various *E. coli* strains down to about 0.03 day^{-1}. Using this approach, a mixed population starting at 1:1 would see the aging strain dominate 10:1 after about 13,000 generations, which would take about 5.3 years. Another factor to consider is that the outcome of such a long competition experiment would likely be determined by other mutations that convey a stronger fitness effect. The relative fitness in the long-term *E. coli* evolution experiment increased to about 1.3 in the first 2000 generations (Lenski and Travisano, 1994). Finally it should be considered that the two strains do not only differ by how they segregate DPAs, but the modifications done (i.e. expression of YFP-Luciferase vs. 2TM-YFP-Luciferase, (Winkler et al., 2010)) may also cause a small difference in the strain's growth rates via other mechanisms (e.g. metabolic cost of protein synthesis). Therefore, it is unlikely that we will be able to observe the fitness benefit of aging in this case. This is a bit disheartening, but it also highlights the utility of the model. It is another case of a model producing information where no observations are possible.

The ecological benefit of aging predicted by our model is consistent with theory and previous models (but see Clegg et al. (2014)). However, it is unlikely that such a small difference would be relevant in the ecology of a gut. Consider the fate of a single cell of the aging phenotype entering a human gut, either by mutation or invasion. Assuming a total population size of 10^{12} (10^{14} total cells, 1% *E. coli* (Consortium, 2012)), an average growth rate of 0.5 day^{-1} (0.2–0.9 day^{-1} (Stein et al., 2013)) and a lifetime of 80 years, that cell would grow to a population of only 50 cells. So the small growth advantage would not support outcompeting the resident population within the lifetime of the host.

From an evolutionary perspective and time scale (bacteria have been evolving for billions of years), even a small fitness benefit is relevant and can support the selection of an aging mutant over a non-aging wild-type. At the low fitness advantage predicted by our model, the fate of an aging mutant would be subject to chance (genetic drift). The probability of a mutation being fixed can be estimated at twice the selection coefficient, so 0.00052 fixations per mutation ((Kimura, 1962), for large populations $N = 10^4$+). However, the large population size and growth rate of bacteria means this may happen frequently. If we assume the aging mutant is the consequence of a single basepair mutation, a mutation rate of 5.4×10^{-10} per division (Drake et al., 1998), then a successful mutant would arise once in every 3.6×10^{12} divisions. In a human gut, with population size and growth rate as above, this many divisions occur every seven days.

It is interesting that the mechanisms responsible for the asymmetric inheritance of damage (aggregation, diffusion and nucleoid occlusion) seem to be passive. This is in contrast to other organisms that segregate damage using active mechanisms. In the *S. cerevisiae*, for example, Hsp104p is involved in the asymmetric damage partitioning (Erjavec et al., 2007). This raises an important question. Did the fitness advantage of this mechanism drive its evolution or is it simply a side effect ("inevitable outcome" (Lele et al., 2011; Watve et al., 2006)) of some other more significant adaptation? For an active, energy-consuming mechanism we would expect it to have evolved as a result of the fitness benefit associated with it. For asymmetric DPA segregation, the small effect on fitness and the passive nature of the mechanisms underlying DPA aging suggest that it is a side effect. In other words, presumably the size and shape of the nucleoid did not evolve to obstruct DPA diffusion and promote their polar localization, but due to other more important reasons. However, experimental evolution experiments suggest that the degree of division asymmetry (in this case observed as differences in offspring generation times) evolves towards increasing fitness, as predicted by a model (Lele et al., 2011; Watve et al., 2006). There are also conflicting reports of active aggregation and polar localization of damage in *E. coli* (Rokney et al., 2009; Winkler et al., 2010). Even if aggregation and polar localization are passive processes, it is clear that some proteins are involved in the aggregation/disaggregation of damaged proteins (Lindner et al., 2008; Winkler et al., 2010), so the cell should have some active control in the overall process. Maybe asymmetric inheritance of DPAs evolved as a side effect, but the degree to which this occurs has been optimized.

4. Summary and outlook

Previous research has established much of the mechanisms underlying aging in *E. coli*, especially as it relates to damaged protein aggregation, diffusion and segregation, but the ecological role of this mechanism has not been explored. We developed a model that explicitly resolves this mechanism by simulating individual DPAs inside the cell, and then simulating a population of such cells. Comparison to relevant data shows that the model is consistent with the main observed patterns. The model predicts that asymmetric inheritance of DPAs results in a small, statistically significant benefit. This is in agreement with theory and other models that show a fitness benefit to asymmetric segregation of damage (but see Clegg et al. (2014)). However, the benefit is small and probably not experimentally measurable or ecologically relevant.

Our conclusion about the fitness benefit emerge from a model designed consistent with the current understanding of the underlying mechanisms and parameterized consistent with the literature; and the model produces patterns consistent with observations. However, we cannot rule out that there is not another model formulation (i.e. different equations) or parameter set that produces an equal-quality calibration (Figs. 2 and 3) but a different result or conclusion about the fitness benefit of asymmetric damage partitioning (Fig. 4). This is a common problem in model prediction and has been referred to as "equifinality" (Beven and Freer, 2001), and it can be addressed to some extent by varying model formulations (Ackermann et al., 2007; Erjavec et al., 2008) and/or parameters (Chen et al., 2004). The present model is computationally very demanding and we were not able to perform this analysis in the present project, but it would be useful to investigate this question in the future.

These results take our understanding of the mechanisms underlying aging in *E. coli* one step further, but it is still far from complete. It is important to reconcile conflicting experimental evidence on aging and passive transport of DPAs in this organism. Another significant knowledge gap at this time is in the "other old pole" aging effect. What is it due to? Some other damage? Or a hardening of the cell wall (Powell and Errington, 1963)? Having multiple mechanisms that contribute to aging is not unusual. In *S. cerevisiae*, for example, oxidative damaged to proteins and accumulation of extrachromosomal DNA circles (ERCs) both contribute to aging (Erjavec et al., 2007; Sinclair, 2002). As with the DPA mechanism, unraveling this mystery has to start with experimental work. *E. coli* is certainly

well-positioned in this regard, as there are numerous fascinating experimental techniques, many of which have already been applied to develop the understanding of the DPA mechanism.

This model increases the amount of mechanistic detail in agent-based models of *E. coli* populations. Future work may expand on this to bring in additional intracellular mechanisms, like metabolism and the function of specific proteins (Hellweger, 2013; Shuler et al., 1979), maybe even at the genome scale (Karr et al., 2012). A natural next step, related to aging, would be to model HSPs and their function (Mogk et al., 2003). Besides serving as a model for aging in bacteria and possibly other organisms, such a model may eventually allow us to provide better understanding and predictions of the ecology of human gut bacteria (Muñoz-Tamayo et al., 2010; Stein et al., 2013) and the environmental fate of pathogens (Bucci et al., 2011; de Brauwere et al., 2011).

This model explicitly combines mechanisms at multiple levels of organization, intracellular and population, which is a common challenge in the biological sciences. Several systems approaches have been developed to address this (Klitgord and Segrè, 2011; Raes and Bork, 2008). The approach used here combines systems biology and systems ecology (which has been referred to as "systems bioecology", (Hellweger, 2010, 2013)). The idea is conceptually quite simple. First, intracellular mechanisms of microorganisms are explicitly simulated (systems biology). Then, whole populations of these individual microbes are simulated (systems ecology). This general approach may be applicable to other questions involving the role of intracellular mechanisms at the population level. The model presented here is unique in that it applies the agent-based approach at both levels of organization. This approach may be useful for simulating other multi-scale situations where the assumption of homogeneity or a continuum may introduce a significant error at the cellular and population levels.

Acknowledgments

We thank Saurabh Mahapatra (MathWorks), Jan Danek (HUMUSOFT), Stefan Savev (Microsoft/ResearchGate) and Jonathon Pendlum (Northeastern U.) for help with the code, Jan-Ulrich Kreft (U. Birmingham) for helpful discussion and advice on modeling aging and Vanni Bucci (U. Massachusetts at Dartmouth) for help with gut bacteria ecology. Two anonymous reviewers provided constructive criticism. This publication is the result of research sponsored by The MIT Sea Grant College Program, under NOAA Grant Number NA10OAR4170086, MIT SG Project Number 2010-R/RT-2/RC-117 and the National Science Foundation (NSF) Grant Number IOS 1121233.

Appendix A. Supplementary data

Supplementary data associated with this article can be found, in the online version, at http://dx.doi.org/10.1016/j.ecolmodel.2015.01.024.

References

Ackermann, M., Stearns, S.C., Jenal, U., 2003. Senescence in a bacterium with asymmetric division. Science 300, 1920.
Ackermann, M., Chao, L., Bergstrom, C.T., Doebeli, M., 2007. On the evolutionary origin of aging. Aging Cell 6, 235–244.
Beven, K., Freer, J., 2001. Equifinality, data assimilation, and uncertainty estimation in mechanistic modelling of complex environmental systems using the GLUE methodology. J. Hydrol. 249, 11–29.
Bray, D., Levin, M.D., Lipkow, K., 2007. The chemotactic behavior of computer-based surrogate bacteria. Curr. Biol. 17, 12–19.
Bucci, V., Hoover, S., Hellweger, F., 2011. Modeling adaptive mutation of enteric bacteria in surface water using agent-based methods. Water Air Soil Pollut., 1–15.
Chao, L., 2010. A model for damage load and its implications for the evolution of bacterial aging. PLoS Genet. 6, e1001076.
Chen, K.C., Calzone, L., Csikasz-Nagy, A., Cross, F.R., Novak, B., Tyson, J.J., 2004. Integrative analysis of cell cycle control in budding yeast. Mol. Biol. Cell 15, 3841–3862.
Clegg, R.J., Dyson, R.J., Kreft, J.-U., 2014. Repair rather than segregation of damage is the optimal unicellular aging strategy. BMC Biol.
Consortium, H.M.P., 2012. Structure, function and diversity of the healthy human microbiome. Nature 486, 207–214.
Coquel, A.-S., Jacob, J.-P., Primet, M., Demarez, A., Dimiccoli, M., Julou, T., Moisan, L., Lindner, A.B., Berry, H., 2013. Localization of protein aggregation in *Escherichia coli* is governed by diffusion and nucleoid macromolecular crowding effect. PLoS Comput. Biol. 9, e1003038.
de Brauwere, A., de Brye, B., Servais, P., Passerat, J., Deleersnijder, E., 2011. Modelling *Escherichia coli* concentrations in the tidal Scheldt river and estuary. Water Res. 45, 2724–2738.
Drake, J.W., Charlesworth, B., Charlesworth, D., Crow, J.F., 1998. Rates of spontaneous mutation. Genetics 148, 1667–1686.
Erjavec, N., Larsson, L., Grantham, J., Nyström, T., 2007. Accelerated aging and failure to segregate damaged proteins in Sir2 mutants can be suppressed by overproducing the protein aggregation-remodeling factor Hsp104p. Genes Dev. 21, 2410–2421.
Erjavec, N., Cvijovic, M., Klipp, E., Nyström, T., 2008. Selective benefits of damage partitioning in unicellular systems and its effects on aging. Proc. Natl. Acad. Sci. 105, 18764–18769.
Evans, M.R., Grimm, V., Johst, K., Knuuttila, T., de Langhe, R., Lessells, C.M., Merz, M., O'Malley, M.A., Orzack, S.H., Weisberg, M., Wilkinson, D.J., Wolkenhauer, O., Benton, T.G., 2013. Do simple models lead to generality in ecology? Trends Ecol. Evol. 28, 578–583.
Fredrick, N.D., Berges, J.A., Twining, B.S., Nuñez-Milland, D., Hellweger, F.L., 2013. Exploring mechanisms of intracellular P heterogeneity in cultured phytoplankton using agent based modeling. Appl. Environ. Microbiol.
Grant, M.A.A., Wacław, B., Allen, R.J., Cicuta, P., 2014. The role of mechanical forces in the planar-to-bulk transition in growing *Escherichia coli* microcolonies. J. R. Soc. Interface 11.
Grimm, V., Revilla, E., Berger, U., Jeltsch, F., Mooij, W.M., Railsback, S.F., Thulke, H.-H., Weiner, J., Wiegand, T., DeAngelis, D.L., 2005. Pattern-oriented modeling of agent-based complex systems: lessons from ecology. Science 310, 987–991.
Hellweger, F.L., 2010. Resonating circadian clocks enhance fitness in cyanobacteria *in silico*. Ecol. Model. 221, 1620–1629.
Hellweger, F.L., 2013. *Escherichia coli* adapts to tetracycline resistance plasmid (pBR322) by mutating endogenous potassium transport: in silico hypothesis testing. FEMS Microbiol. Ecol. 83, 622–631.
Janulevicius, A., van Loosdrecht, M.C.M., Simone, A., Picioreanu, C., 2010. Cell flexibility affects the alignment of model myxobacteria. Biophys. J. 99, 3129–3138.
Johnson, L.R., Mangel, M., 2006. Life histories and the evolution of aging in bacteria and other single-celled organisms. Mech. Ageing Dev. 127, 786–793.
Karr, J.R., Sanghvi,.C., Macklin, D.N., Gutschow, M.V., Jacobs, J.M., Bolival, B., Assad-Garcia, N., Glass, J.I., Covert, M.W., 2012. A whole-cell computational model predicts phenotype from genotype. Cell 150, 389–401.
Kimura, M., 1962. On the probability of fixation of mutant genes in a population. Genetics 47, 713–719.
Kirkwood, T.B.L., 2005. Understanding the odd science of aging. Cell 120, 437–447.
Klitgord, N., Segrè, D., 2011. Ecosystems biology of microbial metabolism. Curr. Opin. Biotechnol. 22, 541–546.
Kreft, J.-U., Booth, G., Wimpenny, J.W.T., 1998. BacSim, a simulator for individual-based modelling of bacterial colony growth. Microbiology 144, 3275–3287.
Lele, U.N., Baig, U.I., Watve, M.G., 2011. Phenotypic plasticity and effects of selection on cell division symmetry in *Escherichia coli*. PLoS ONE 6, e14516.
Lenski, R.E., Travisano, M., 1994. Dynamics of adaptation and diversification: a 10,000-generation experiment with bacterial populations. Proc. Natl. Acad. Sci. 91, 6808–6814.
Lenski, R.E., Simpson, S.C., Nguyen, T.T., 1994. Genetic analysis of a plasmid-encoded, host genotype-specific enhancement of bacterial fitness. J. Bacteriol. 176, 3140–3147.
Lindner, A.B., Madden, R., Demarez, A., Stewart, E.J., Taddei, F., 2008. Asymmetric segregation of protein aggregates is associated with cellular aging and rejuvenation. Proc. Natl. Acad. Sci. 105, 3076–3081.
Melke, P., Sahlin, P., Levchenko, A., Jönsson, H., 2010. A cell-based model for quorum sensing in heterogeneous bacterial colonies. PLoS Comput. Biol. 6, e1000819.
Mogk, A., Deuerling, E., Vorderwülbecke, S., Vierling, E., Bukau, B., 2003. Small heat shock proteins, ClpB and the DnaK system form a functional triade in reversing protein aggregation. Mol. Microbiol. 50, 585–595.
Muñoz-Tamayo, R., Laroche, B., Walter, É., Doré, J., Leclerc, M., 2010. Mathematical modelling of carbohydrate degradation by human colonic microbiota. J. Theor. Biol. 266, 189–201.
Pedraza, J.M., van Oudenaarden, A., 2005. Noise propagation in gene networks. Science 307, 1965–1969.
Powell, E.O., Errington, F.P., 1963. Generation times of individual bacteria: some corroborative measurements. J. Gen. Microbiol. 31, 315–327.
Raes, J., Bork, P., 2008. Molecular eco-systems biology: towards an understanding of community function. Nat. Rev. Microbiol. 6, 693–699.
Rang, C.U., Peng, A.Y., Chao, L., 2011. Temporal dynamics of bacterial aging and rejuvenation. Curr. Biol. 21, 1813–1816.
Rokney, A., Shagan, M., Kessel, M., Smith, Y., Rosenshine, I., Oppenheim, A.B., 2009. *E. coli* transports aggregated proteins to the poles by a specific and energy-dependent process. J. Mol. Biol. 392, 589–601.

Rudge, T.J., Steiner, P.J., Phillips, A., Haseloff, J., 2012. Computational modeling of synthetic microbial biofilms. ACS Synth. Biol. 1, 345–352.
Saberi, S., Emberly, E., 2010. Chromosome driven spatial patterning of proteins in bacteria. PLoS Comput. Biol. 6, e1000986.
Shuler, M.L., Leung, S., Dick, C.C., 1979. A mathematical model for the growth of a single bacterial cell. Ann. N.Y. Acad. Sci. 326, 35–52.
Sinclair, D.A., 2002. Paradigms and pitfalls of yeast longevity research. Mech. Ageing Dev. 123, 857–867.
Stein, R.R., Bucci, V., Toussaint, N.C., Buffie, C.G., Rätsch, G., Pamer, E.G., Sander, C., Xavier, J.B., 2013. Ecological modeling from time-series inference: insight into dynamics and stability of intestinal microbiota. PLoS Comput. Biol. 9, e1003388.
Stewart, E.J., Madden, R., Paul, G., Taddei, F., 2005. Aging and death in an organism that reproduces by morphologically symmetric division. PLoS Biol. 3, e45.
Volfson, D., Cookson, S., Hasty, J., Tsimring, L.S., 2008. Biomechanical ordering of dense cell populations. Proc. Natl. Acad. Sci. 105, 15346–15351.
Wang, P., Robert, L., Pelletier, J., Dang, W.L., Taddei, F., Wright, A., Jun, S., 2010. Robust growth of *Escherichia coli*. Curr. Biol. 20, 1099–1103.
Watve, M., Parab, S., Jogdand, P., Keni, S., 2006. Aging may be a conditional strategic choice and not an inevitable outcome for bacteria. Proc. Natl. Acad. Sci. 103, 14831–14835.
Winkler, J., Seybert, A., Konig, L., Pruggnaller, S., Haselmann, U., Sourjik, V., Weiss, M., Frangakis, A.S., Mogk, A., Bukau, B., 2010. Quantitative and spatio-temporal features of protein aggregation in *Escherichia coli* and consequences on protein quality control and cellular ageing. EMBO J. 29, 910–923.